Electronic Supplementary Material (ESI) for Journal of Materials Chemistry A.

Supporting Information

Morphology Control of Low Temperature Fabricated ZnO Nanostructures for Transparent Active Layers in All Solid-State Dye-Sensitized Solar Cells

*Kun Wang, Volker Körstgens, Dan Yang, Nuri Hohn, Stephan V. Roth, Peter Müller-Buschbaum**

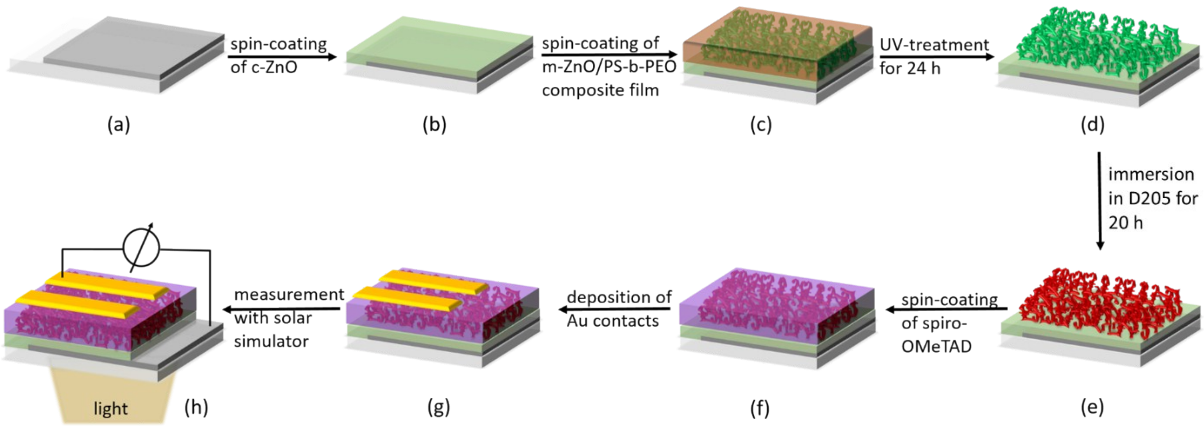

Figure S1. Schematic representation of the different steps involved in the fabrication of an all solid-state dye-sensitized solar cell based on the nanostructured ZnO films.

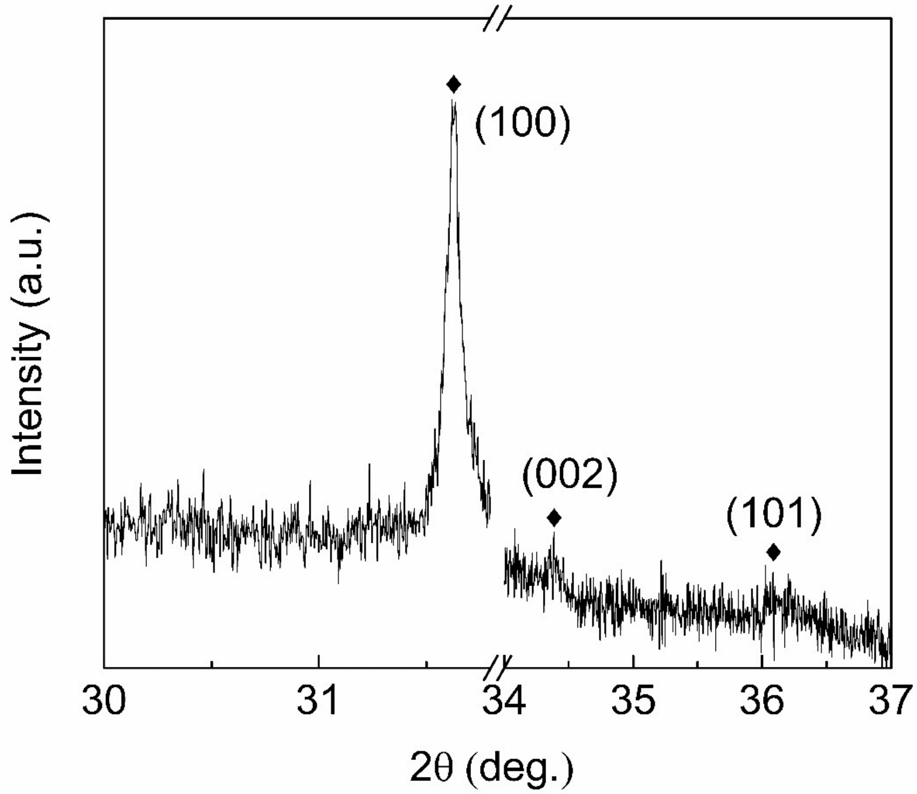

Figure S2. XRD pattern of mesoporous ZnO film annealed at 80 °C after polymer removal. The Bragg peaks at 31.6, 34.4, and 36.1 deg correspond to crystal planes of (100), (002) and (101), respectively. The curve is interrupted from 32.5 to 34 deg to remove the strong Bragg peak of the Si substrate. The Bragg peaks of ZnO wurtzite phase are indicated by diamonds.

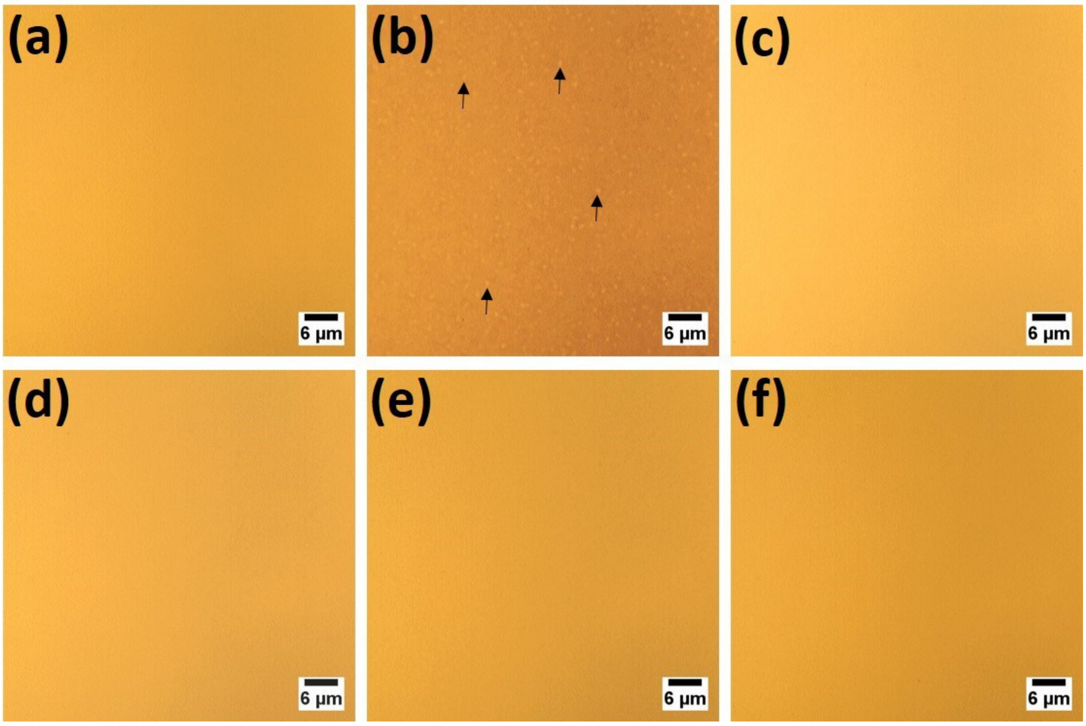

Figure S3. OM images of mesoporous ZnO films annealed at different temperatures after polymer removal: (a) 80 °C, (b) 100 °C, (c) 120 °C, (d) 140 °C, (e) 160 °C, and (f) 200 °C. Black arrows in (b) indicate some of the light spots, implying large scale aggregation.

GISAXS data modeling

In order to extract quantitative information on the lateral thin film structure from the horizontal line cuts, the GISAXS data are modeled in the framework of the effective interface approximation of the distorted wave Born approximation (DWBA) using the local monodisperse approximation (LMA). This means that the total scattering signal can be approximated by incoherently superposing the scattering intensities of the individual substructures that appear within the film, if the length scales of the distinct substructures are sufficiently different. In our model, three such distinct substructures are approximated by standing cylinders with Gaussian distribution for the form and structure factors (Figure S4). The form factors denote the shape of these scattering objects in the film which in the present case is ascribed to the ZnO clusters. The diameters of these cylindrical objects obtained from the fits denote the size of the ZnO clusters. The structure factors obtained from the fits, on the other hand, account for the center-to-center distance between the scattering objects.[1, 2] Values of the form and the structure factors are then used to extract the average pore size of the ZnO films:

Pore size = (centre-to-centre distance between the nanoparticles - 2 x radius of the clusters).

Based on these calculations, the cluster sizes and pore sizes of the mesoporous ZnO film are obtained.

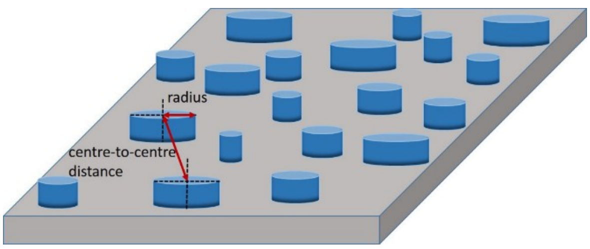

Figure S4. Sketch of the scattering objects morphology. In the framework of the local monodisperse approximation, only objects belonging to the same substructure contribute to the total scattering signal.

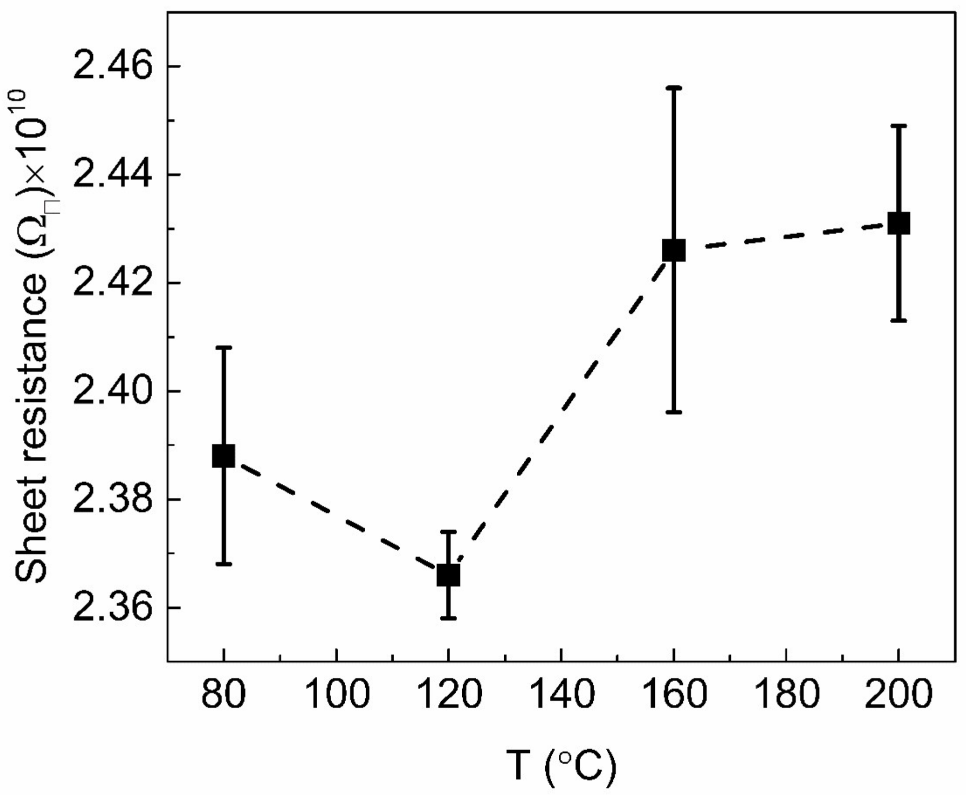

Figure S5. Sheet resistance of mesoporous ZnO films prepared at different annealing temperatures as indicated. The dashed line is a guide to the eyes.

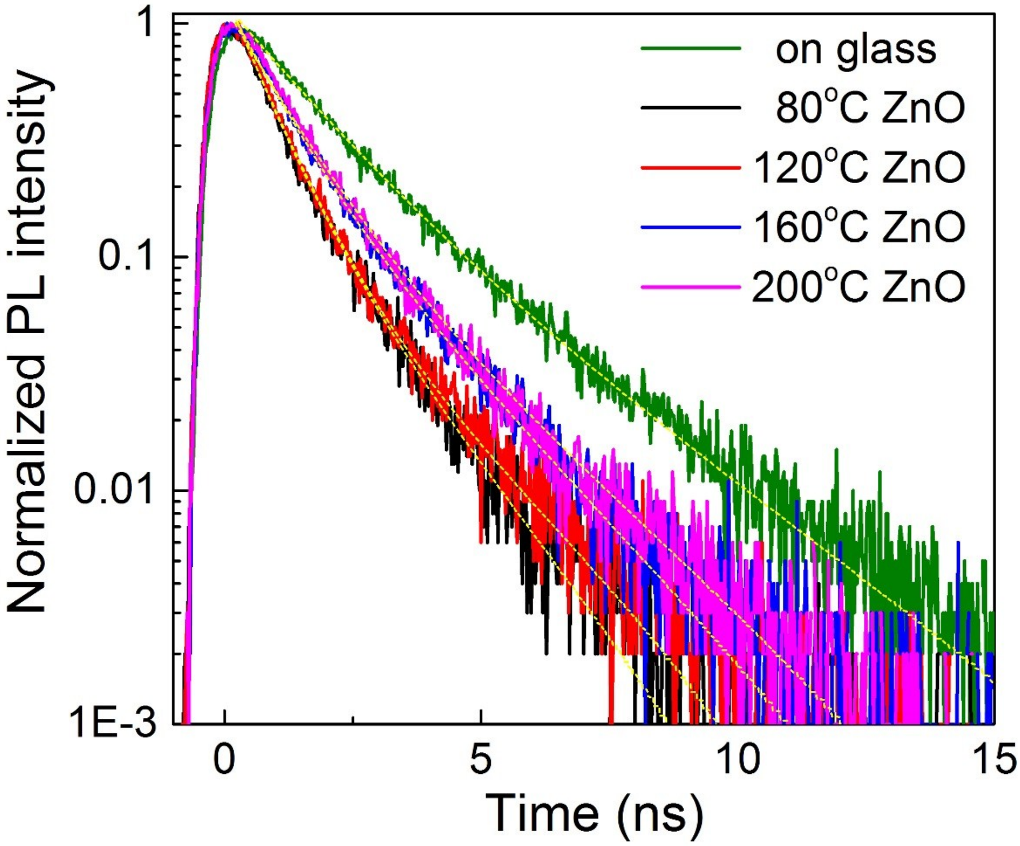

Figure S6. Time resolved PL spectra of D205 on glass and on mesoporous ZnO films prepared at different annealing temperatures as indicated. The curves are fitted with biexponential decay function to obtain the average lifetime. The fits are shown as dashed yellow lines.

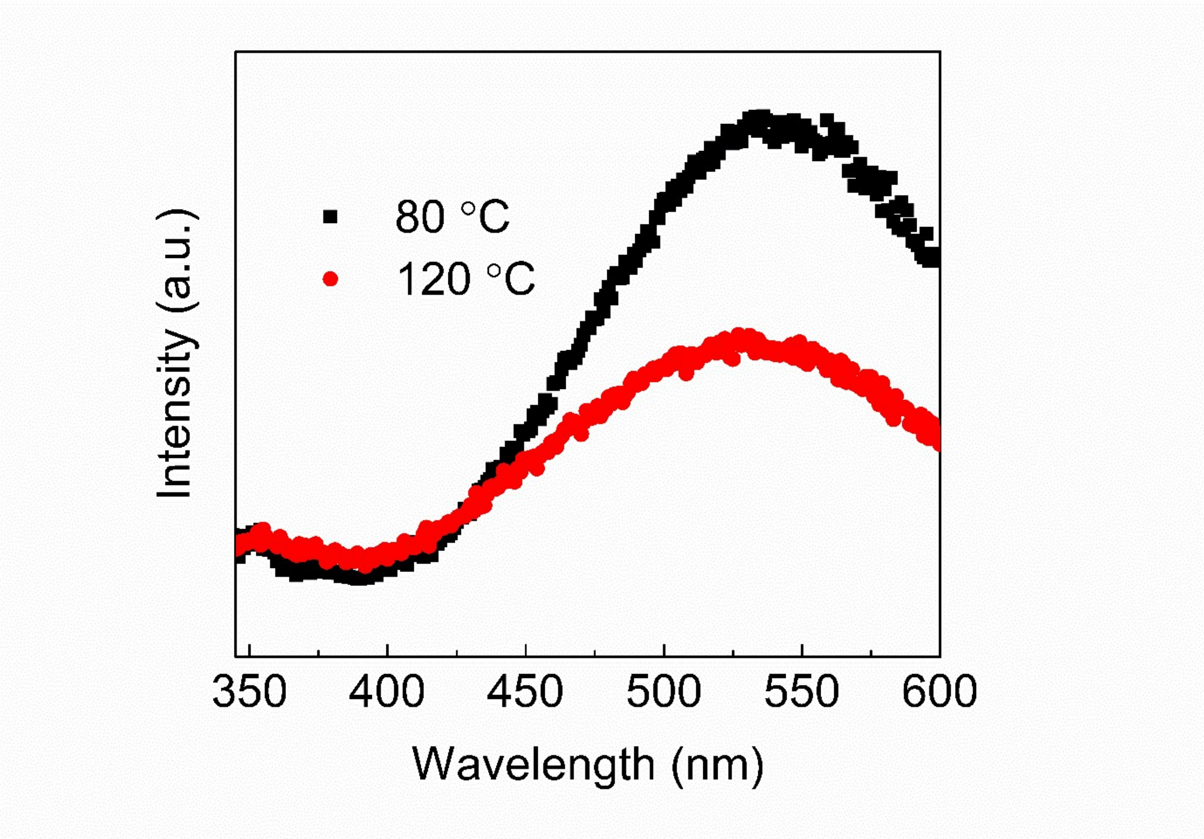

Figure S7. PL spectra of mesoporous ZnO films annealed at 80 and 120 °C after polymer removal (λ_{Ex}=325 nm). Peaks at about 350 nm are caused by the radiative recombination of electrons from the conduction band with holes from the valence band. While the other broad peaks located at about 530 nm may be resulted from some defects induced emission.

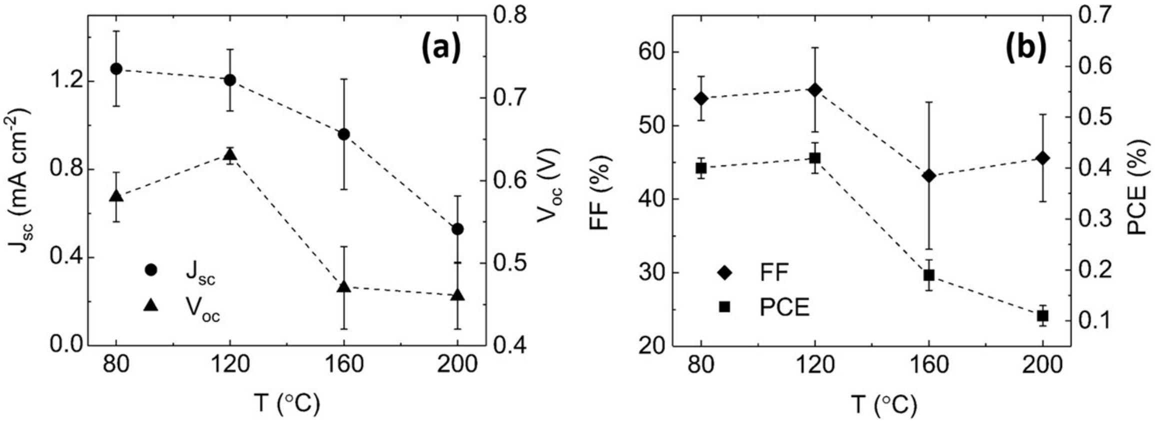

Figure S8. (a) J_{sc} (circles, dataset at the top) and V_{oc} (triangles, dataset at the bottom), (b) FF (diamonds, dataset at the top) and PCE (squares, dataset at the bottom) extracted from J-V curves of the DSSCs based on ZnO prepared at different annealing temperatures as indicated. The lines are guides to the eye.

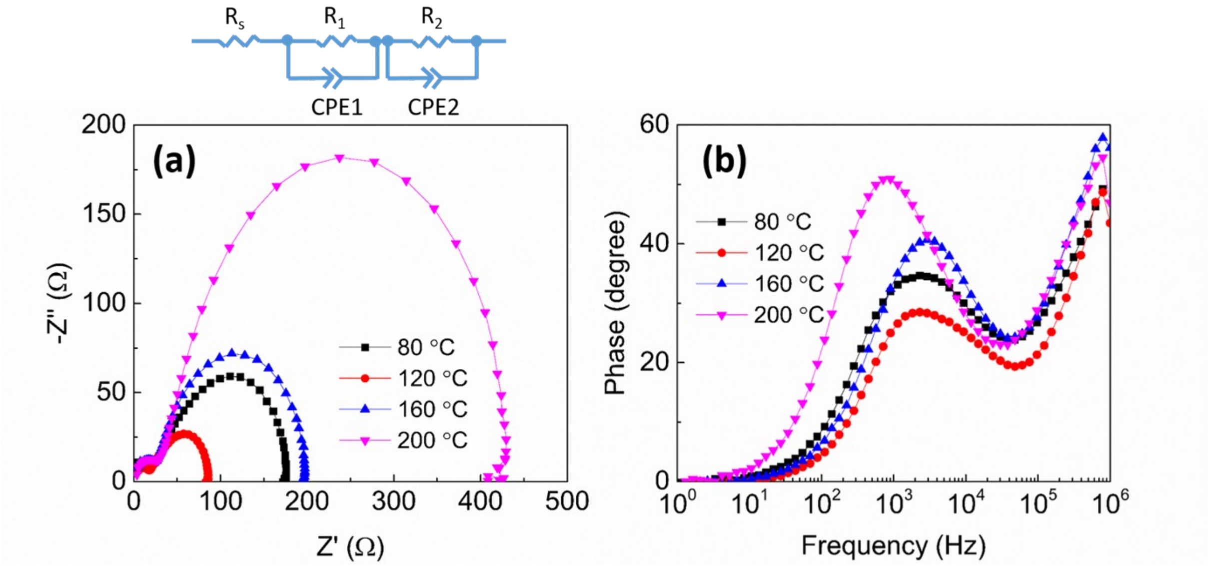

Figure S9. EIS analyses of DSSCs based on ZnO prepared at different annealing temperatures as indicated. (a) Nyquist plots (inset showing equivalent circuit model used for the DSSCs in this study). (b) Bode phase plots.

Table S1. EIS parameters of DSSCs based on ZnO prepared at different annealing temperatures as indicated.

devices based on different ZnO films	R_1 (Ω)	R_2 (Ω)	f_{max} (Hz)	τ (ms)
80 °C	25.2	153.6	2302	0.069
120 °C	20.7	65.4	1823	0.087
160 °C	28.5	170.1	2910	0.055
200 °C	29.4	403.7	905	0.180

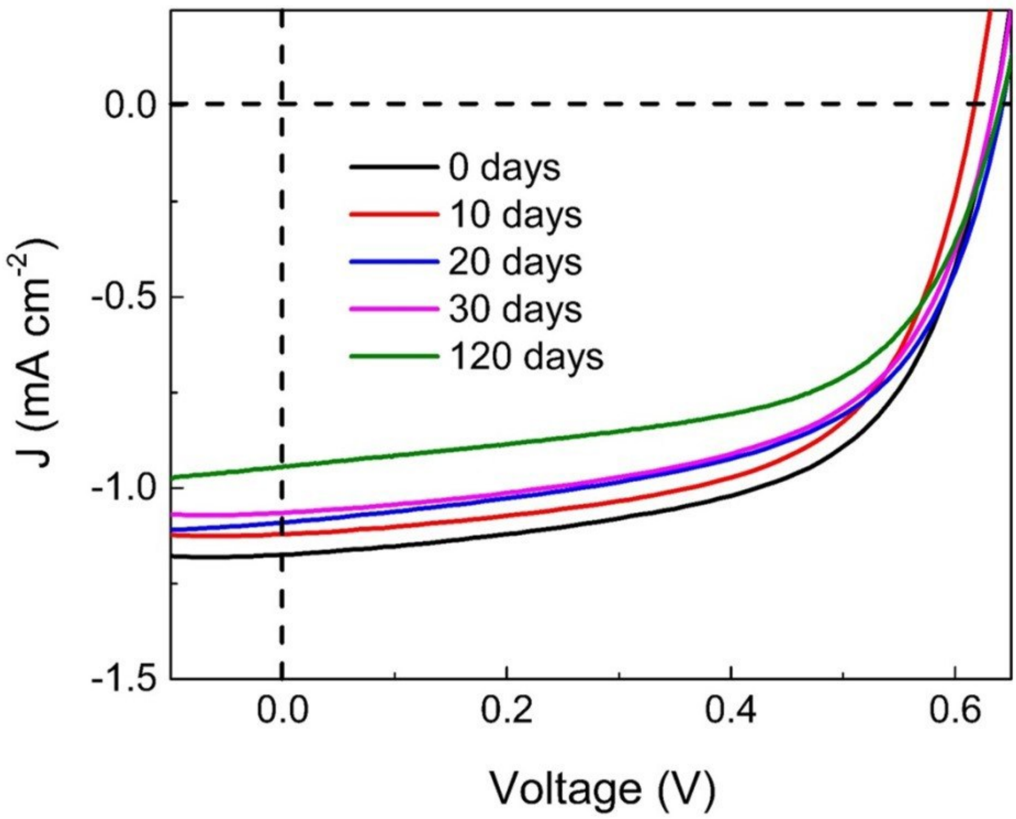

Figure S10. Current-voltage characteristics of all ssDSSC based on ZnO film annealed at 120 °C after several days in ambient air conditions.

References:

[1] M. Rawolle, K. Sarkar, M. A. Niedermeier, M. Schindler, P. Lellig, J. S. Gutmann, J.-F. Moulin, M. Haese-Seiller, A. S. Wochnik, C. Scheu and P. Müller-Buschbaum, *ACS Appl. Mater. Interfaces* 2013, **5**, 719.

[2] R. Lazzari, *J. Appl. Crystallogr.* 2002, **35**, 406.